LOAD APPLICATION AND CONTROL SYSTEMS UTILIZED TO SIMULATE COMBINED LOADS ENVIRONMENTS FOR SATURN V - APOLLO SPACECRAFT

George Shipway
Wyle Laboratories
Norco, California

A combined-loads test program was conducted on the Service Module, Spacecraft Lunar Module Adapter, Lunar Module, Instrument Unit, and SIVB Forward Skirt, to prove the structural integrity of the Short-Stack segment of the Saturn V - Apollo Spacecraft structure to the severe loading at Max Q Alpha and End Boost flight phases. Both localized and distributed, static equivalents of thrust, maneuver, aerodynamic and dynamic loads were simulated by means of hydraulically powered loading linkages and large air bladders. These static loading systems were designed to add a minimum of constraint to the test specimen, which was dynamically excited at the Service Module and the Lunar Module. A real-time thermal environment was applied to the SIVB by means of a zoned array of quartz lamps to reproduce skin temperatures and radial thermal gradients. Semi-automatic control systems were utilized in all cases to provide accurate and rapid control of each of the simulated loads. This included provisions for uniformly increasing static loads in increments of constant percent design load, real-time control and tracking of thermal loads, and damped load release methods for rapid dumping of static loads in the event of any system or structural failure. This paper describes the engineering techniques, loading mechanisms, and control systems employed to achieve these combined load environments.

INTRODUCTION

The launch of the Saturn V space vehicle imposes various combinations of loads on the entire spacecraft structure. The spacecraft is designed to withstand these extremes of static and dynamic mechanical loads, aerodynamic loads, and temperature variations, however, during the second Saturn V flight, evidence of unexpected structural degradation was encountered.

This test program, identified as the "Integrated Shell Static Structural Test" was designed to demonstrate the structural integrity of the structure, as an assembly. The assembled structure provided realistic boundary conditions not possible when the component stages were tested individually. The expedited test program was to subject the "Short Stack" portion of the Saturn V to the two most critical environments encountered during the thrust of the first stage. The two test conditions simulate "Max Q Alpha" (maximum product of dynamic pressure and angle of attack), and "End of Boost" where the maximum axial acceleration and near maximum temperature on the structure occur.

This test program was a joint effort between Wyle Laboratories, NASA, and the five stage contractors which included North American Rockwell (Tulsa and Downey Divisions), Grumman Aircraft Engineering Corporation, McDonnell Douglas Corporation, and International Business Machines Corporation.

The test program was conducted at Wyle Laboratories Huntsville Facility.

For further information on this test program, the reader is referred to Reference 1.

DESCRIPTION OF TEST SPECIMEN

The Saturn V Apollo Integrated "Short Stack" test specimen consisted of five major assemblies. The assemblies were the Service Module, The Spacecraft Lunar Module Adapter, the Lunar Module, the Instrument Unit, and the SIVB Forward Skirt. For reference, please see Figure 1, which illustrates the short stack in relation to the whole Saturn V vehicle.

The Service Module (SM) for this test program included only the primary structure. The forward struts which normally mate to the Command Module were removed to facilitate the interfacing with the Dummy Command Module. The loads generated by the fuel and oxidizer tanks were simulated with loading fixtures which will be described later. The mission of the Service Module in this test program was to accept the loads applied by the loading devices to be described and to properly distribute these loads into the Spacecraft Lunar Adapter, i.e., it was considered a loading structure rather than part of the test specimen. The static weight of the SM was approximately 4,000 lbs.

The Spacecraft Lunar Adapter (SLA) was essentially complete. The static weight of the SLA was approximately 3,600 lbs.

The Lunar Module (LM) was structurally complete. All of the significant components were installed or mass simulated. The fuel and oxidizer tanks were loaded with liquids to their proper static weight. The four landing gear struts were not included. The total weight of the LM was 28,760 lbs.

The Instrument Unit (IU) was structurally complete, and all of the components were mass simulated. The weight of the IU was approximately 4,500 lbs.

The SIVB Forward Skirt (SIVB) was structurally complete. The forward tank bulkhead was not included, but the skirt was mounted to a 9 inch adapter section which approximately simulated the radial support of the bulkhead. None of the components normally attached to the inside of the skirt were mounted or simulated. The weight of the SIVB was approximately 1,500 lbs.

As assembled, the overall height of the specimen was approximately 55 feet, and the base diameter was 22 feet. The static weight was approximately 42,400 lbs.

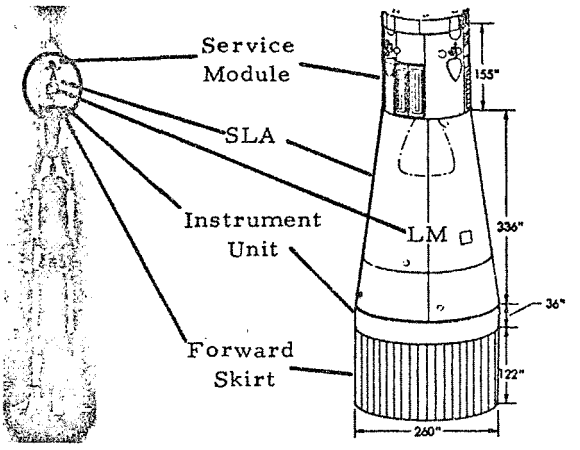

Figure 1. Short Stack Test Configuration Compared to Saturn V - Apollo Vehicle

LOAD REQUIREMENTS

The test requirements called for loading the specimen with combinations of static and dynamic mechanical loads, simulated aerodynamic loads, and temperature. The two test conditions, Max Q Alpha and End Boost, each called for particular combinations of static and dynamic loading in terms of axial, shear, and bending moments. For each test condition, the loading was applied in two ways. In one, the static loads, with an additional static equivalent of dynamics, were applied in percentage increments to ultimate loads (140% of Design or Limit loads). In the second, the static loads were applied to 100% or Limit load values and held while the dynamic loading was applied. Figures 2 and 3 indicate the axial, shear, and bending moment loads as appropriate to each condition. The loads indicated are the maximum static loads applied, i.e., they are ultimate loads and include the static equivalent for dynamics. The loads resulting from the application of aerodynamic pressure during Max Q Alpha are also included. The temperature requirements, which applied only to the SIVB and only during End Boost condition, will be presented later. The dynamic loading requirements, small compared to the static loads, will also be presented later.

STATIC LOADING DEVICES

All of the static loading devices included three elements in series, i.e., a hydraulic cylinder, a load cell, and an air spring. The rationale behind this design will be discussed later. Starting at the top of the "stack" each of the static loading devices will be described.

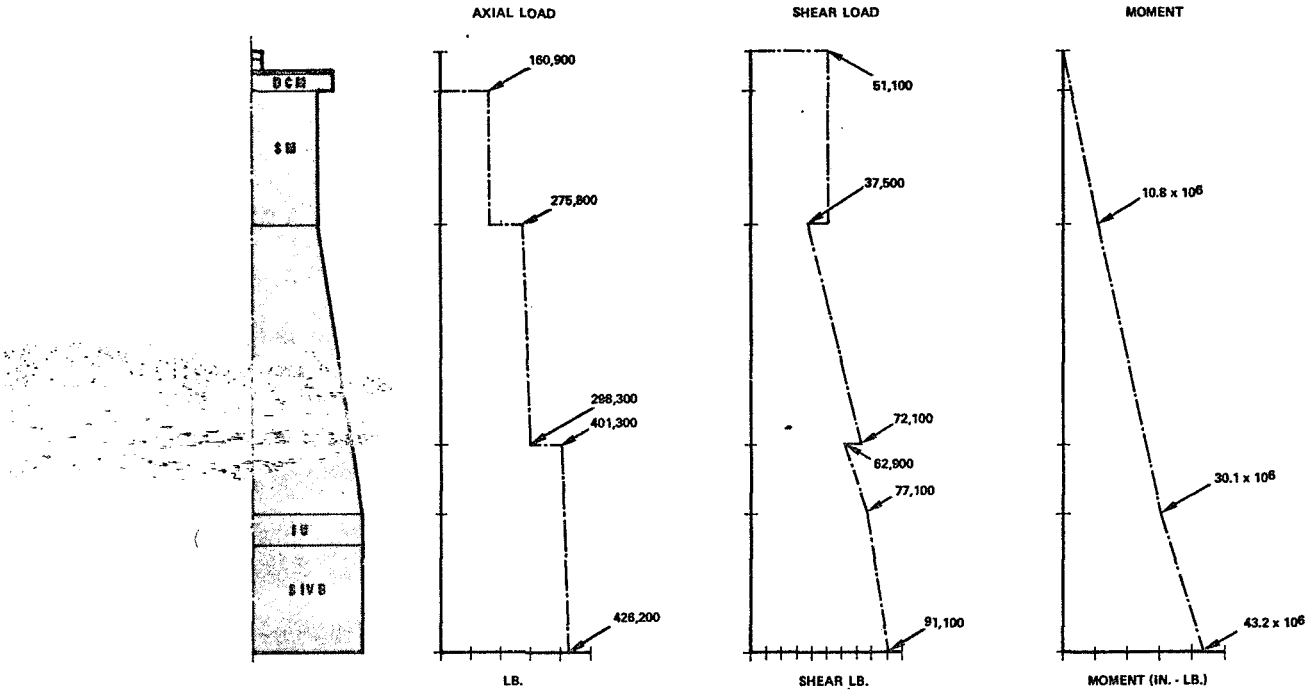

Figure 2. Max Q Alpha Ultimate Load Requirements

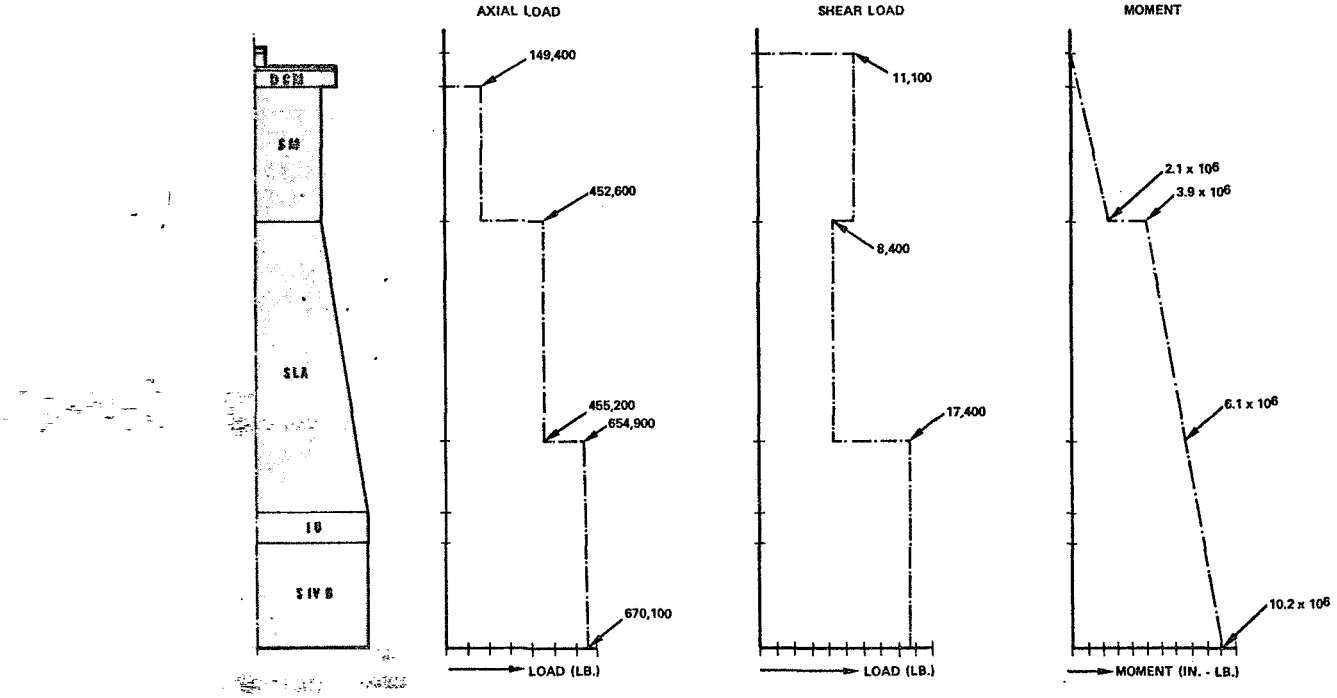

Figure 3. End Boost Ultimate Load Requirements

Dummy Command Module

As already mentioned, the forward end of the Service Module interfaced with a load fixture which was designated the Dummy Command Module. Figure 4 illustrates the DCM in position on top of the Service Module. For applying axial load, the DCM interfaced with the Service Module at twelve locations corresponding to the inner and outer ends of each of the six SM radial shear field beams. The main fixture loaded the outer ends of the radial beams, and a secondary fixture loaded the inner ends of the beams. Figure 5 (looking forward through the center section of the Service Module) illustrates the secondary fixture in position on the inner ends of the radial beams. The DCM shear loading was transmitted to the Service Module through a circumferential angle member attached to the outside surface of the Service Module.

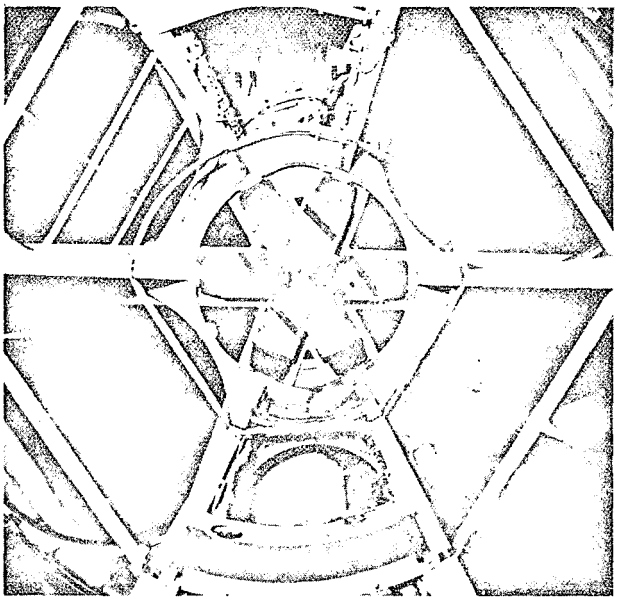

Figure 4. Dummy Command Module In Position on Top of Service Module

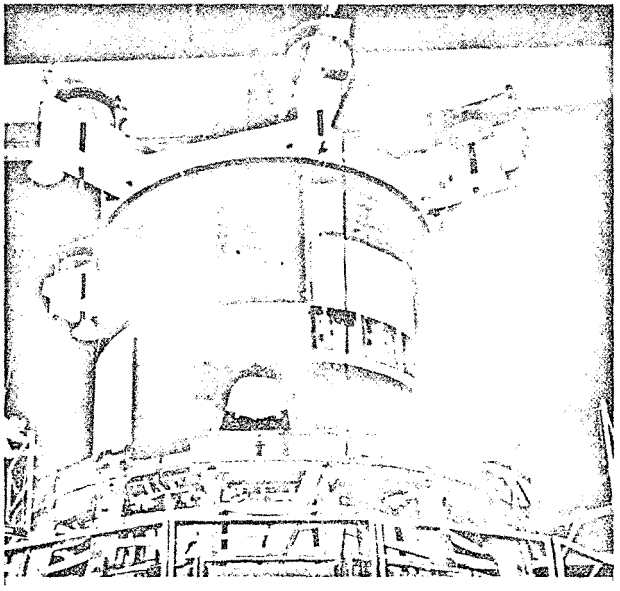

Figure 5. DCM Secondary Loading Fixture, View Forward from Inside Service Module

Figure 6 is a schematic showing load vectors representing the various loads applied to the DCM. In this and the following schematics the load vectors are shown to illustrate the maximum magnitude of the loads applied at various points. Note, however, that the loads were applied to satisfy the load diagrams previously shown and were not necessarily all at their maximum value at the same time.

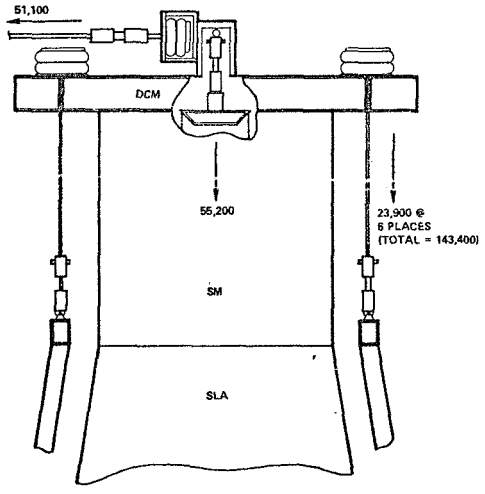

Figure 6. DCM Load Schematic

Axial loads were applied to the ends of each of the six spokes of the DCM through 28 inch diameter air springs as seen in Figure 7. Below the air springs are the tension rods, load cells, and hydraulic cylinders. Hidden in the center tube of the DCM is the hydraulic cylinder and load cell that applied 35 percent of the DCM axial load to the secondary fixture. A shear load was applied to the DCM through a shear loading mechanism around the square center column of the DCM. Its vertical posi-

tion was selected to yield the desired moment at the aft interface of the SM. The spokes of the DCM were 24 inch x 120 lb. wide flange beams. The DCM weighed 16,600 lbs.

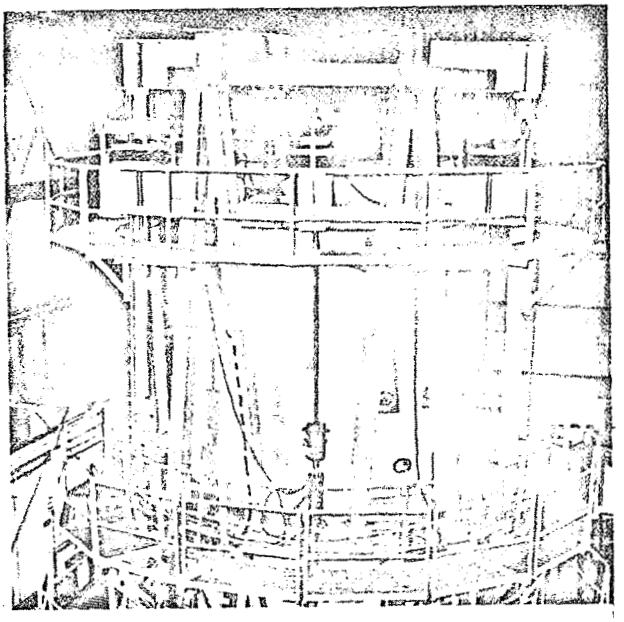

Figure 7. DCM Static Loading Mechanisms

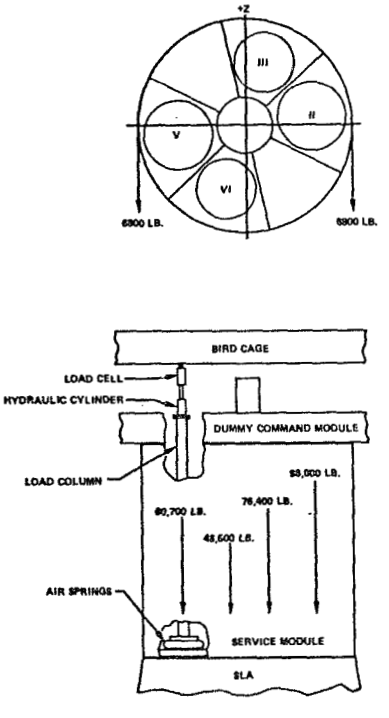

Figure 8. Service Module Load Schematic

SM Tank Loaders

Four of the six sectors of the Service Module contain fuel and oxidizer tanks which represent a large portion of its weight. Accordingly, it was desirable to simulate the tank loads. Figure 8 schematically illustrates the tank loads. The bottom of the SM sector was covered with a 3 inch thick aluminum plate to distribute the load. On the plate was mounted three 22.4 inch diameter air springs as seen in Figure 9. The center of the three-spring pattern was positioned 5 inches outboard of the normal tank centerline to provide a more realistic load distribution. The three-spring groups were loaded with "telephone poles" (8 inch pipe) topped with hydraulic actuators as seen in Figure 10. Above the hydraulic actuators were the load cells.

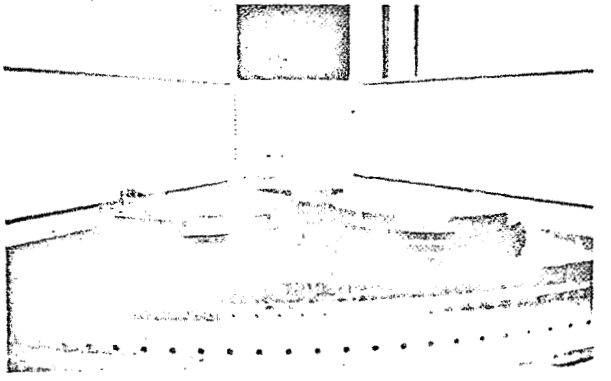

Figure 9. Tank Loader Air Springs in Service Module - outer skin panel removed

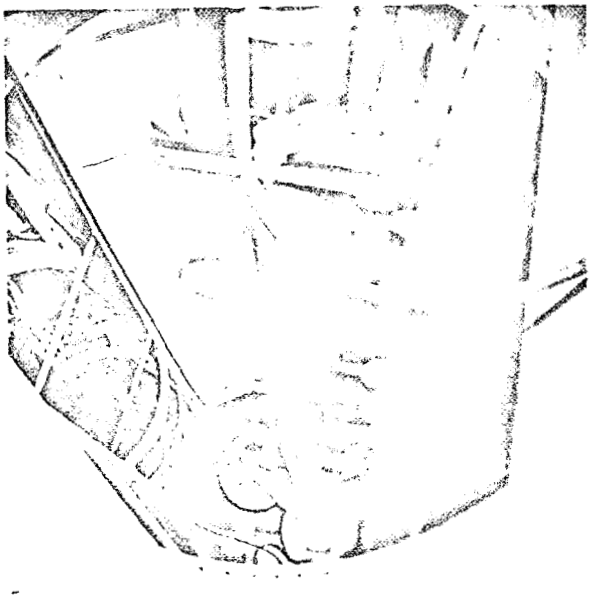

Figure 10. Tank Loading Struts

SM Shear Loaders

A negative shear load was required at the interface between the Service Module and the SLA as shown schematically in Figure 8. The loads were applied by attaching two tangential straps to the sides of the Service Module just above the interface with the SLA as seen in Figure 11. Figure 12 shows the load cell, and 13 inch air spring used at this position. Hidden behind the air spring is the hydraulic cylinder.

SLA Air Bladders

To simulate the aerodynamic loading associated with the Max Q Alpha condition, the conical surface of the SLA was covered with air bladders. The circumference was divided into sixteen 22-1/2° segments for ease in controlling the circumferentially varying pneumatic pressure loading, and for ease of fabrication and installation of the bladders. As seen in Figure 13, the bladders were also separated at the level of the LM support fittings to allow access to the SLA at that point. Figure 14 illustrates one of the upper SLA bladders during leak testing. The bladders were fabricated from neoprene impregnated nylon to withstand a maximum pressure of 2.5 psig within the restraint provided by the setup. Figure 15 schematically illustrates the loading from the air bladders. The asymetrical pressure distribution resulted in a net positive shear load of 48,800 pounds. Even though the maximum pressure applied was only 1.65 psig, the total crushing load on the SLA was 178,000 pounds.

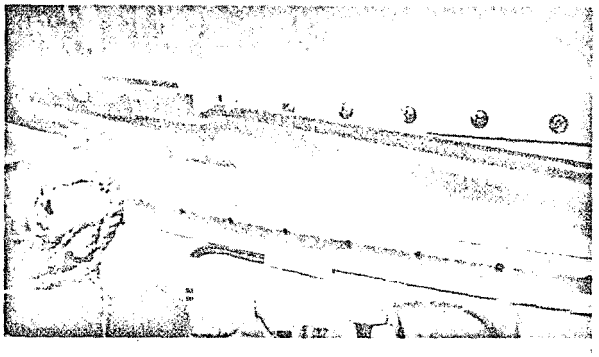

Figure 11. Service Module Shear Load Attachment

Figure 12. Service Module Shear Loader

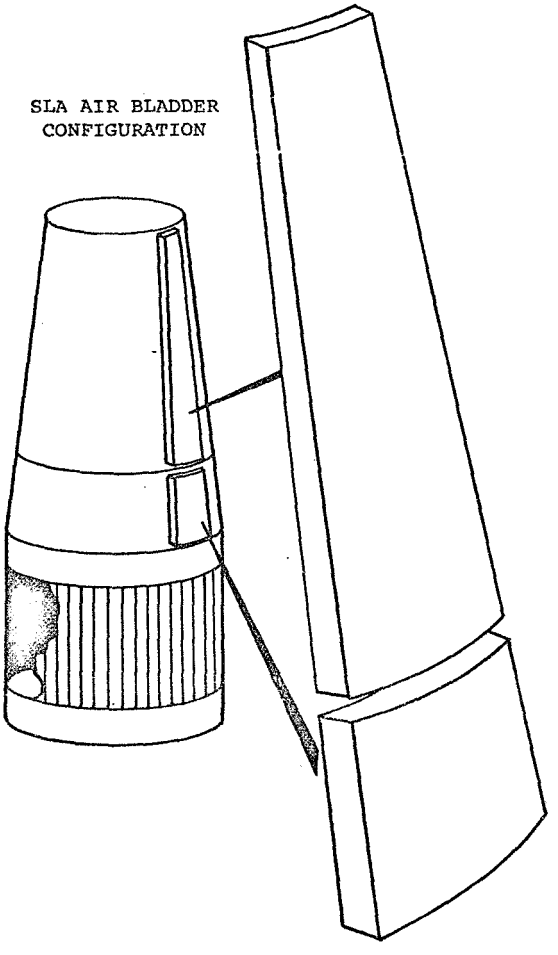

Figure 13. SLA Air Bladder Arrangement

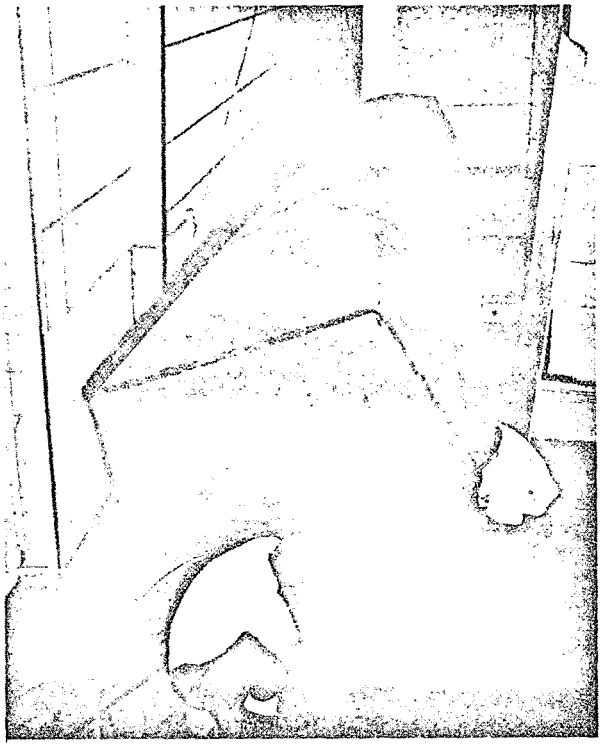

Figure 14. SLA Air Bladder during Leak Testing

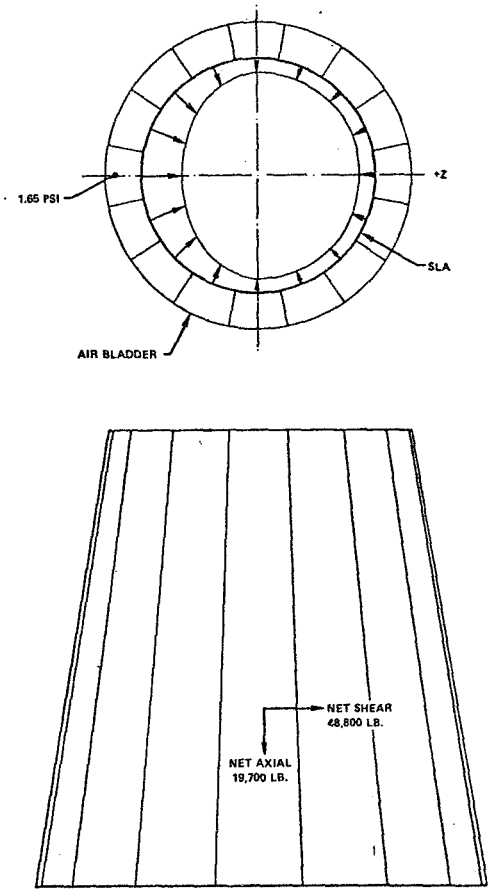

Figure 15. SLA Pressure Load Schematic

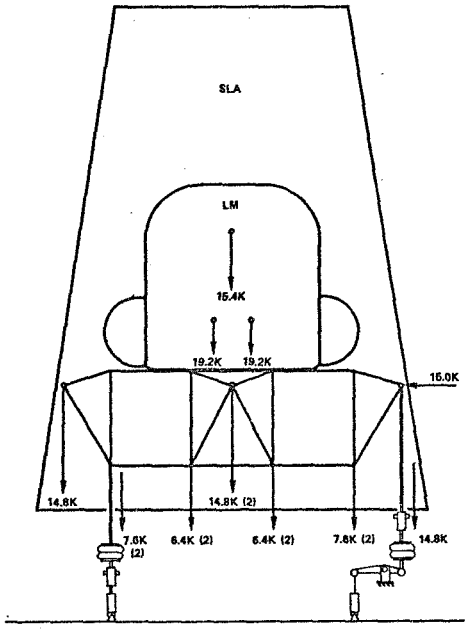

Figure 16. Lunar Module Load Schematic

LM Loaders

Sixteen static loads were applied to the LM. Figure 16 schematically illustrates the loading. A compressive shear load was applied at one of the Apex fittings (where the LM attaches to the SLA). An axial load was applied near each of the four apex fittings where the landing gear strut normally attached. This loading device partially shown in Figure 17 consisted of a load cell (not shown), a 17.4 inch air spring, a lever and a hydraulic cylinder. The lever mechanism was necessary because of space limitations. Three tension rods were overlapped inside of these air springs to enable them to apply a tension load. Axial loads were applied to each of the eight corners of the descent stage. As partially illustrated in Figure 18, these loaders were a 13 inch diameter air spring, load cell, and hydraulic cylinder combination. It can be seen here that the air spring was enclosed in a "cage" to enable the spring to apply a tension load.

Figure 17. Lunar Module Apex Loader

Figure 18. Lunar Module Corner Loader

Three of the LM axial loads were attached to the ascent stage, one to a fixture mounted in the forward access tunnel, and two to a

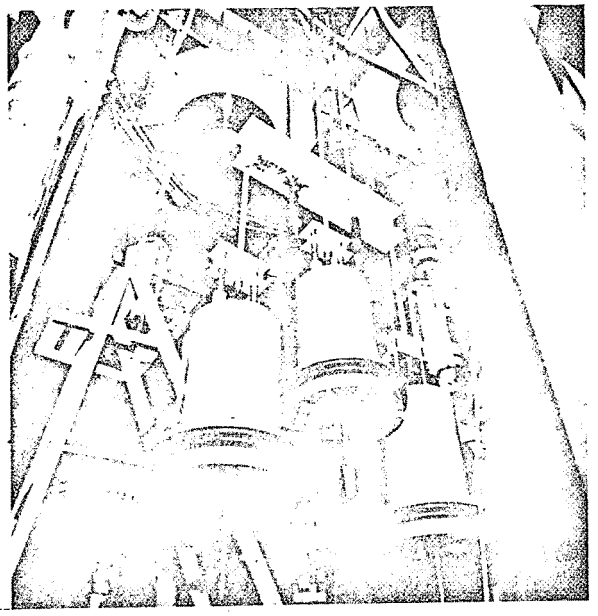

Figure 19. Lunar Module Ascent Stage Loaders

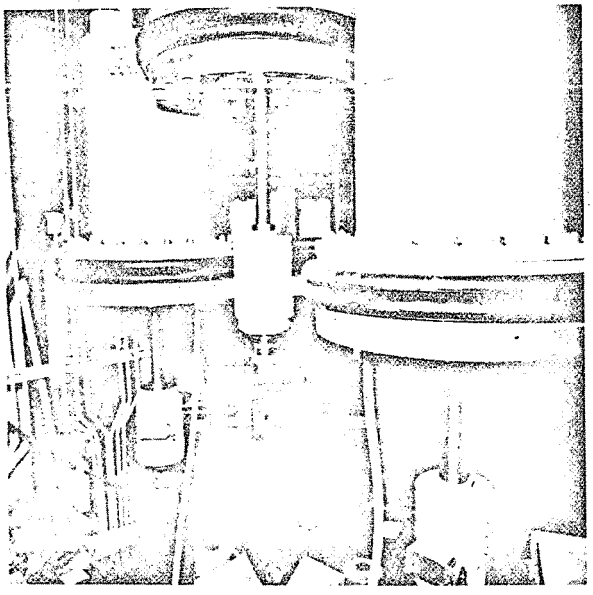

Figure 20. Lunar Module Ascent Stage Loaders

fixture lower in the stage. Tension rods were brought down through the space normally occupied by the ascent and descent stage engines, and connected to air springs, as seen in Figure 19. Figure 20 shows the lower end of these three loading assemblies. The large air reservoirs attached to these three air springs will be discussed later.

IU Loaders

Eight axial loads were attached to nine of the heavier dummy components inside the Instrument Unit. Figure 21 is a schematic presentation of the loads. Figure 22 illustrates two of the loading mechanisms. Due to clearance requirements for the SIVB air bladders below, it was necessary that all components of the IU loading mechanisms stay above the aft plane of the IU. To accomplish this, all the IU loaders operated as compression loaders in the horizontal position through bell cranks to apply the axial tension loads to the components.

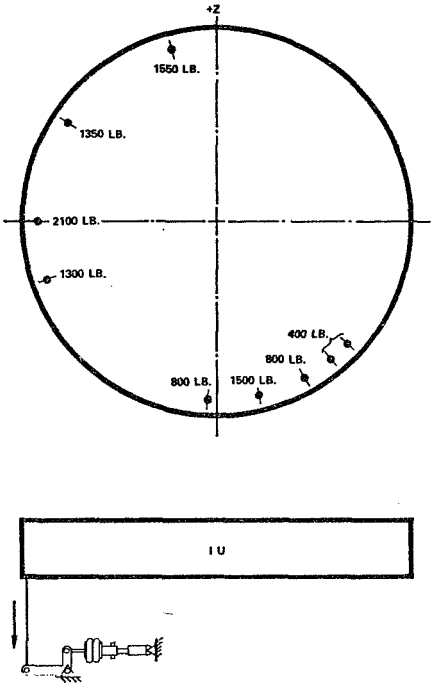

Figure 21. Instrument Unit Load Schematic

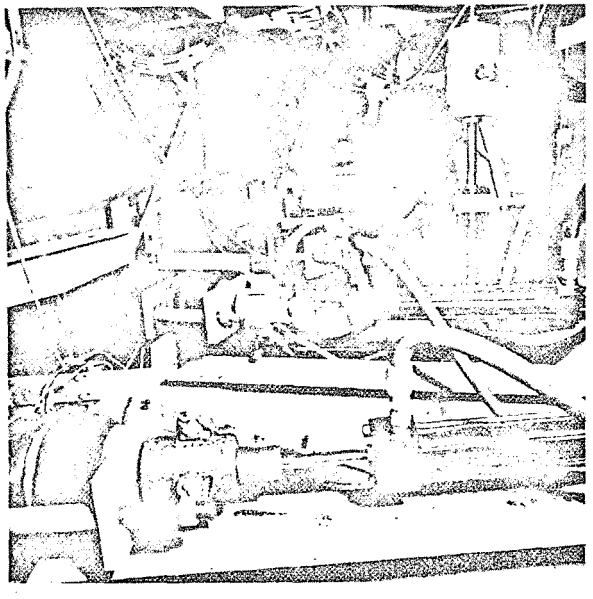

Figure 22. Instrument Unit Comp nent Loaders

SIVB Bladders

During the Max Q Alpha testing, air bladders were installed inside the SIVB forward skirt to simulate the negative aerodynamic loading on the skin. Figure 23 schematically shows the loading on the skirt. In a similar fashion to the SLA bladders, these bladders were separated into sixteen segments around the inside of the skirt. They were further separated into three bands fore and aft to facilitate matching the interior structure of the skirt as seen in Figure 24. The maximum pressure applied was 1.33 psig which resulted in a total expanding force of 116,000 pounds.

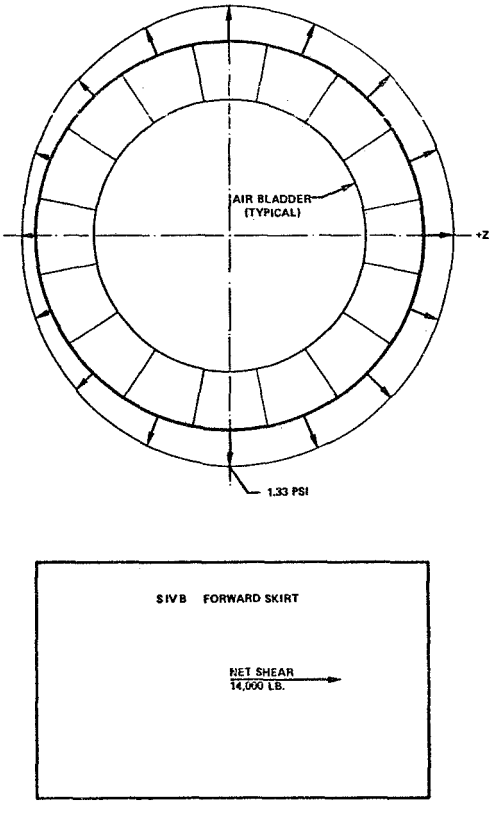

Figure 23. SIVB Pressure Load Schematic

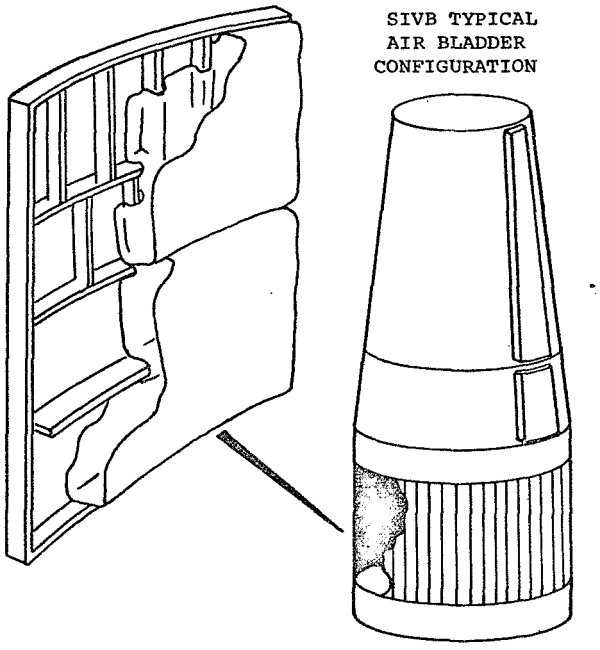

Figure 24. SIVB Air Bladder Arrangement

SIVB Heaters

During the End Boost phase of the testing, quartz heat lamps were installed around the SIVB Skirt to simulate aerodynamic heating.

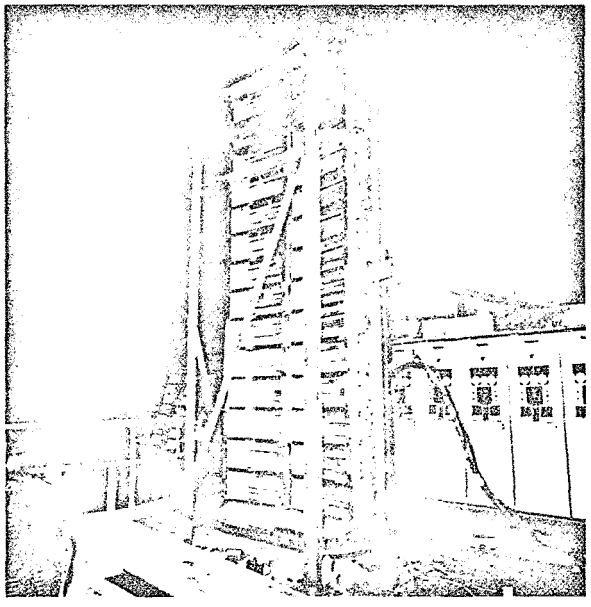

Figure 25. Quartz Lamp Panel for Heating SIVB

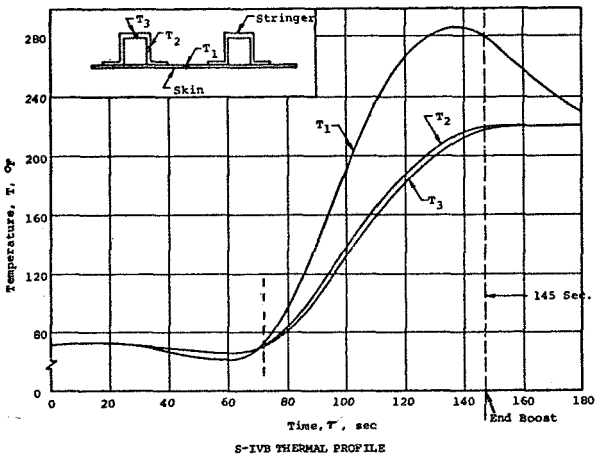

Figure 26. SIVB Thermal Profile

Figure 25 shows two banks of heat lamps. Three hundred thirty-six heating units, each with three 2500 watt lamps were required to cover the area. These banks of heat lamps were installed approximately 1 ft. away from the skin of the SIVB around the entire circumference. A polished aluminum sheet barrier, at the level of the SIVB-IU interface, limited the air convection currents to minimize the heat transmitted to the upper stages of the stack. Figure 26 illustrates the required temperature time history and temperature gradients for the SIVB Skirt skin and stringers.

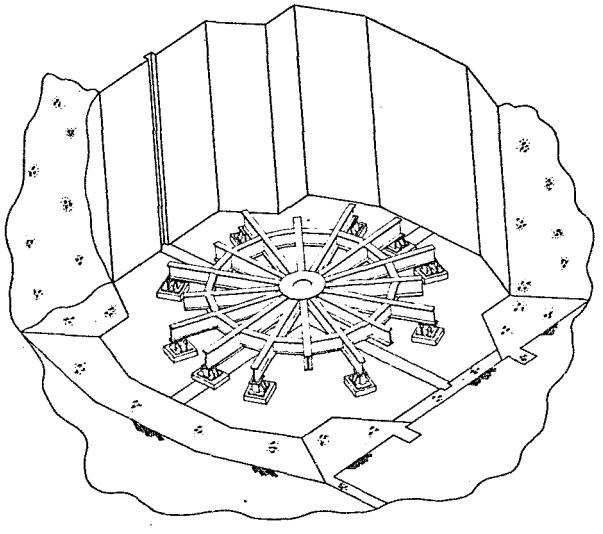

Figure 27. Base Frame

LOAD RESTRAINT STRUCTURES

Base Frame

The entire assembly was supported on the base frame. The 34 ft. diameter frame was fabricated of 24 inch x 160 lb. wide flange beam as illustrated in Figure 27. The frame was fabricated in the bottom of the 26 ft. deep pit and was anchored at the ends of ten spokes to existing hydrashaker mounting pads which, in turn, are part of a 1 million pound reaction mass. The frame was designed to support and restrain, with a minimum of deflection, the axial, shear, and bending moment loads applied to the specimen; to provide a reasonably uniform support under the circumference of the specimen; and to support and anchor the various loading fixtures attached to it. The total axial loads reacted directly into the base frame were 1, an upload of 421,900 lbs. by the bird cage; 2, a down load of 597,100 lbs. by the specimen; 3, an upload of 121,500 lbs. by the lion cage; and 4, an upload of 53,700 lbs. in the center.

External Structure

All of the external loads were reacted into the bird cage shown in Figure 28. The lower section of the cage served to transmit the loads from the upper sections to the base frame, and to support the quartz lamp units during end boost testing. This section of the bird cage was fabricated outside and moved into the pit in one piece. The cage was supported by the floor and held down by the base frame.

The middle or conical section of the cage received supplemental lateral support at floor level from 16 horizontal beams. The 15,000 lb. shear load at the LM Apex fitting was supported and guided by the bird cage with help from a horizontal beam to the pit wall just below floor level. The top beam of the conical section reacted the axial loads applied to the six spokes of the DCM (143,300 lbs. total). The two shear loads applied to the bottom of the Service Module were also reacted into the top beam of the conical section. This section of the bird cage was fabricated and assembled outside, split into halves, moved inside, and assembled around the specimen.

The upper section of the bird cage restrained the axial tank loads (282,000 lbs. total). The upper section also supported and guided the 51,000 lb. shear load applied to the top of the DCM. A large part

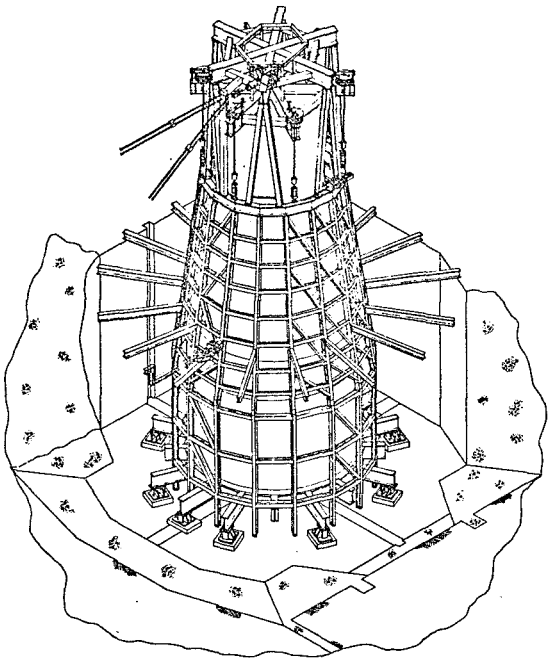

Figure 28. Bird Cage Load Restraint Structure

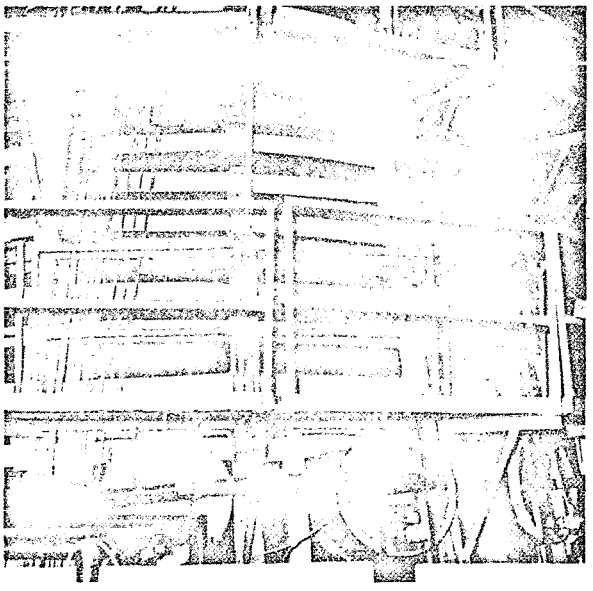

Figure 29. SLA Bladder Restraint

of the restraint of this load was taken by four one inch back stay rods sloping down to an adjacent reaction mass. The spokes of the top section were 24 inch x 120 lb. wide flange beams.

The mid-section of the bird cage also supported the air bladders which applied the

air loads to the SLA. Figure 29 shows a portion of the bladder restraining system. The white bands are 6 inch wide nylon straps which provided the support for the bladders between the vertical beams of the cage. The large openings in the bladders, which will be discussed later, were closed with trash can lids into which the air supply and control lines were installed. A two inch pipe framework attached to the inside of the bird cage provided the top, bottom, and side restraints for the SLA air bladders.

Internal Structure

The three axial loads, applied to the ascent stage of the LM (53, 700 lb. total), were reacted directly into the center of the base frame. All other internal loads were reacted into the lion cage. The 12 descent stage loading mechanisms and the IU loading mechanisms all attached to the top beam of the lion cage. The sixteen legs of the lion cage attached to the top of the base frame members, and transmitted to the base the 121, 500 lb. axial load. Figure 30 shows the lion cage being lowered into position inside the stack. To provide support for the inside diameter of the SIVB air bladders, the outside diameter of the cage was wrapped with 1/8 inch cable with a spacing of about 4 inches. A 2 inch pipe framework attached to the cage provided the barrier between segments of the air bladders. The top and bottom surfaces of the bladders were restrained with plywood panels.

The other major internal structure was the monkey cage. The function of this cage was to support the displacement measuring transducers, and, accordingly, it carried no load. The design criteria for this cage was to be as stiff as practical without exceeding the very severe space limitations within the stack. Figure 31 shows the lower section of the monkey cage installed. The outer ends of the radial members supported the upper section of the monkey cage, part of which is seen in Figure 32. Figure 32 is indicative of the

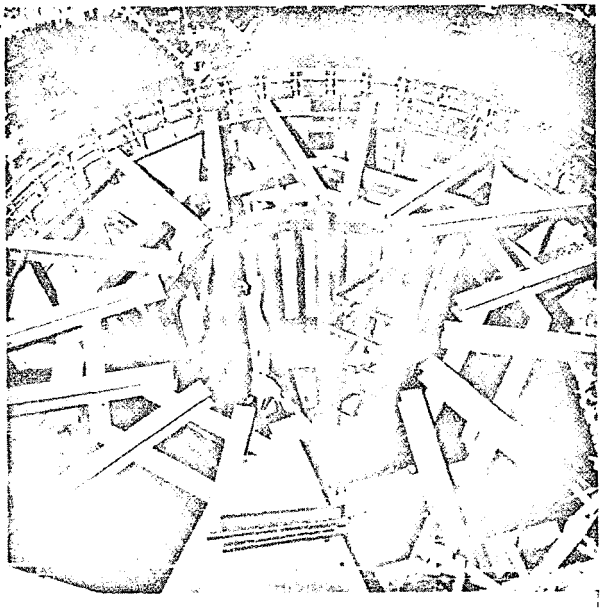

Figure 31. Lower Monkey Cage in Position

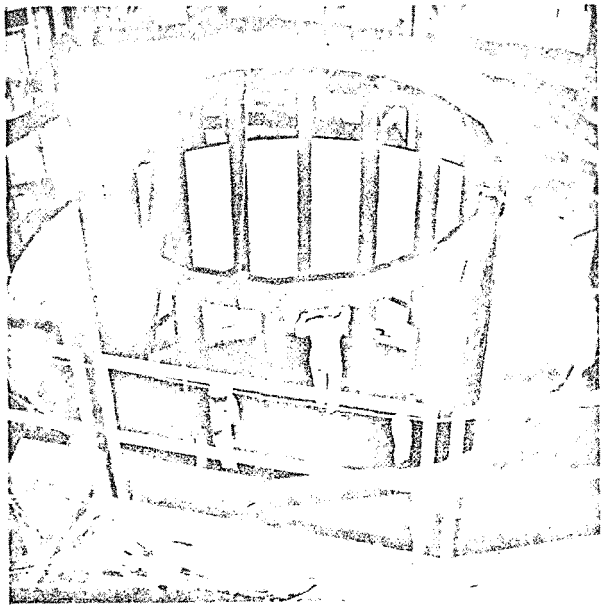

Figure 30. Lion Cage Being Lowered into Position

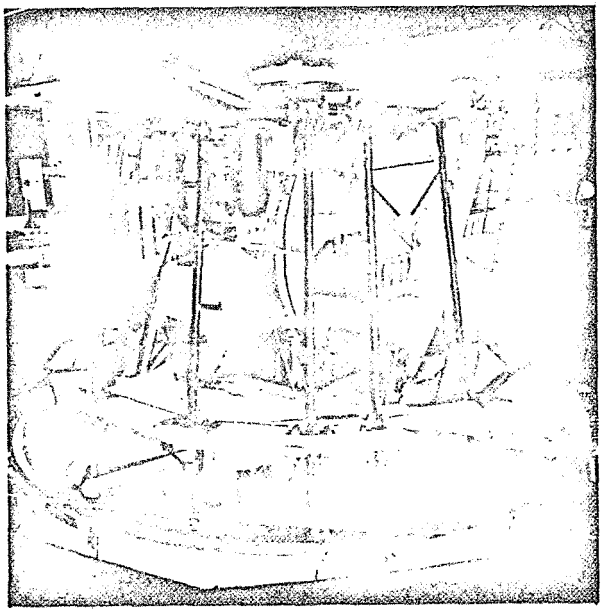

Figure 32. Portion of Upper Monkey Cage in Position around LM

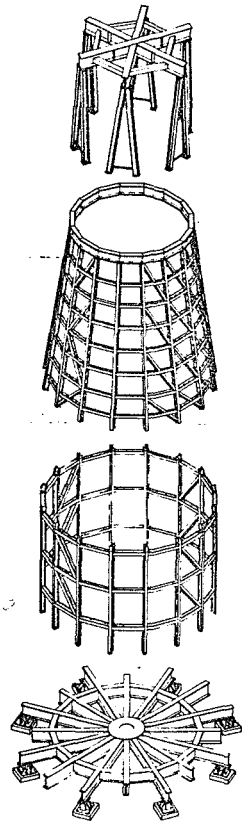

Figure 33. External Load Restraint Structure

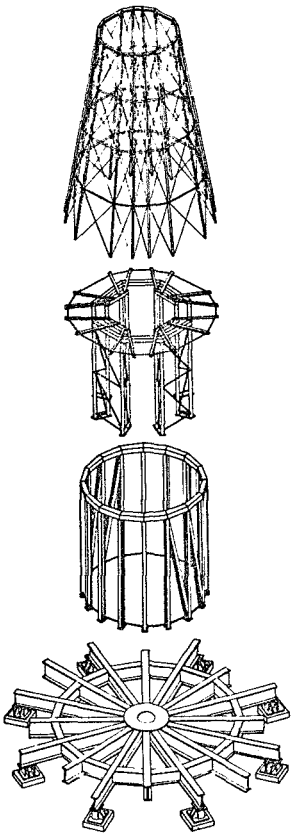

Figure 34. Internal Structure

severe space restrictions imposed on the design and fabrication of the upper section where it was necessary to stay safely inside the SLA, but stay safely away from the LM. The upper section of the monkey cage continued up to within 6 inches of the top of the SLA.

Figures 33 and 34 present exploded composites of the external and internal structures.

DYNAMICS

DCM Shakers

The test required the application of dynamic loading to the DCM and to the LM. The frequency range of interest was from five Hz to ten Hz. The dynamic axial loads were applied to the DCM just inside the static load points on the lower side of three of the spokes. The mechanism was a hydraulic actuator, driving the DCM, which was reacted through a column and a load cell to an 18,000 lb. reaction mass. The reaction mass was suspended by air springs from the upper bird cage. The actuator was driven through a hydraulic servo valve with phase and amplitude control provided between the three systems. The horizontal dynamic load was applied to the DCM in the Z direction in a similar fashion except that the 6,000 lb. reaction mass was pendulum supported from the bird cage. Figure 35 shows the setup for dynamics loading. The design capacity of the shakers was about 6,000 lbs. each for the axial direction and about 2,000 lbs. for the horizontal direction.

During the checkout of the dynamics system an instability problem between the three axial shakers appeared. When a solution to the problem was not quickly forthcoming, the schedule forced the decision to delete the dynamics from the DCM and add a static equivalent load to the static loading.

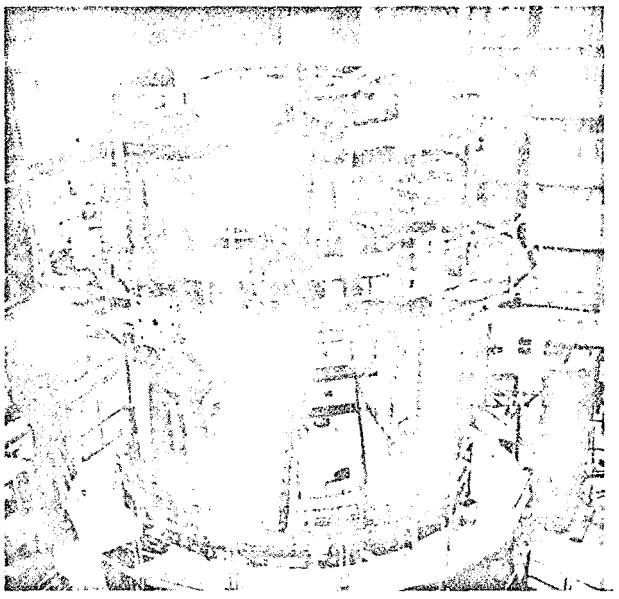

Figure 35. DCM Dynamic Loading Setup

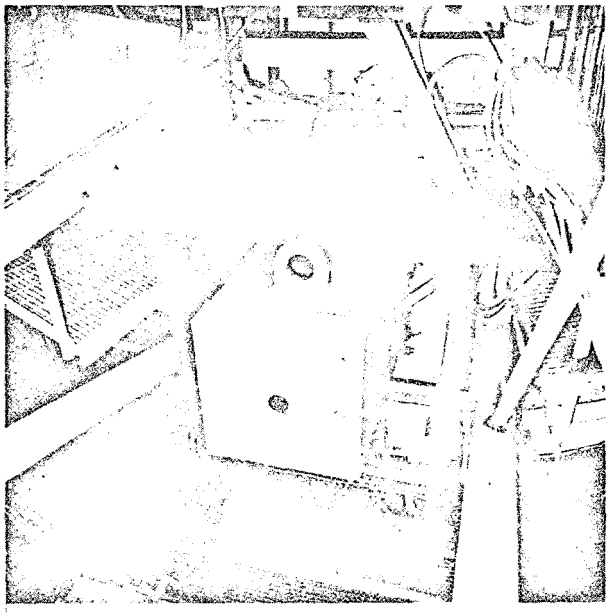

Figure 36. Reaction Mass for Dynamic Load applied to Lunar Module Apex

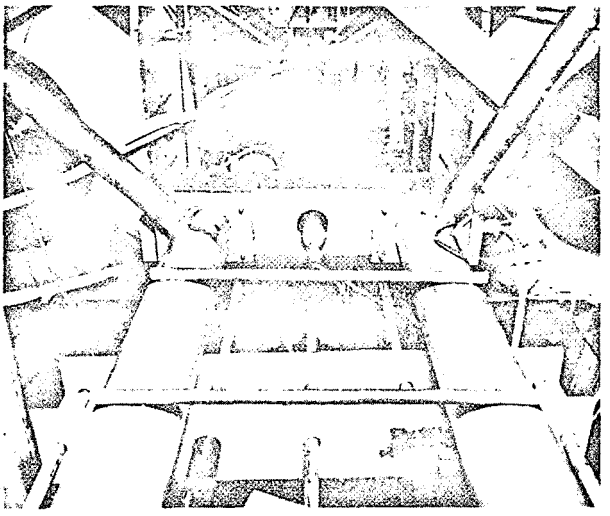

Figure 37. Lunar Module Dynamic Axial Loading Structure

Figure 38. Lunar Module Dynamic Axial Loading Cylinders

LM Shakers

The dynamic loads to the LM were applied as a horizontal load into one of the apex fittings, and as axial loads into each of the two descent engine thrust struts. The design load capacity for each of the shakers was about 2,000 lbs., however, during the test substantially less force than that was used. As seen in Figure 36, the reaction block for the horizontal exciter was pendulum supported from the bird cage. Figures 37 and 38 show the axial loading exciters, tubular drive stingers, and support structure which was reacted directly into the base frame. The two axial actuators were excited from a single small servo valve.

DESIGN AND CONTROL CONSIDERATIONS

Static Load Systems

The design of the static loading mechanisms followed, more or less, conventional static loading practice. Each loader consisted of a hydraulic cylinder, a load cell, and an air spring, in series with suitable mechanical linkages. Figure 39 schematically illustrates the static loading system. The hydraulic cylinders were "off the shelf" design and sizes for fast delivery. The use of hydraulic cylinders permitted precise control of loads and ample stroke capability. The cylinders were all selected to operate as near to 2500 psi at full load as standard sizes would permit. The Edison controllers permitted precise and convenient control of the loads in terms of percent of limit load regardless of the individual hydraulic pressures required. Figure 40 shows the four Edison controller units ganged together to operate from a single control. The load cells permitted precise electrical readout of the loads applied, and were compatible with the instrumentation system.

The departure from standard static technique was in the use of the air spring. The requirement for dynamic testing dictated that the loading devices must not contribute any significant stiffness to the test structure since such stiffness would change the dynamic response of the specimen and invalidate the test results. A second reason was that without a soft spring, there could have been large fluctuations in the static loads. The inclusion of the air springs in the loading mechanism provided the low stiffness desired. The three static loads attached to the ascent stage of the LM were expected to see the greatest dynamic motion and were in a position to seriously affect the axial dynamic response of the LM. To further reduce the stiffness of these three air springs they were provided with relatively large air reservoirs as seen in Figure 19.

The air springs were required during dynamic testing, but would be somewhat of a nuisance during the static phases of the test. Therefore, each air spring was provided with a mechanical stop which permitted the spring to be overpressurized and effectively eliminated from the circuit during the static phases of the test. Prior to the dynamic portions of the test, the air springs were adjusted to a pre-selected pressure which would position them in approximately mid stroke when the required static load was applied. Each air spring was equipped with a microswitch near each end of its stroke which would illuminate a pilot light and call for a fine pressure adjustment if the spring was not near mid-stroke after static load application. The air pressures were manually and individually controlled.

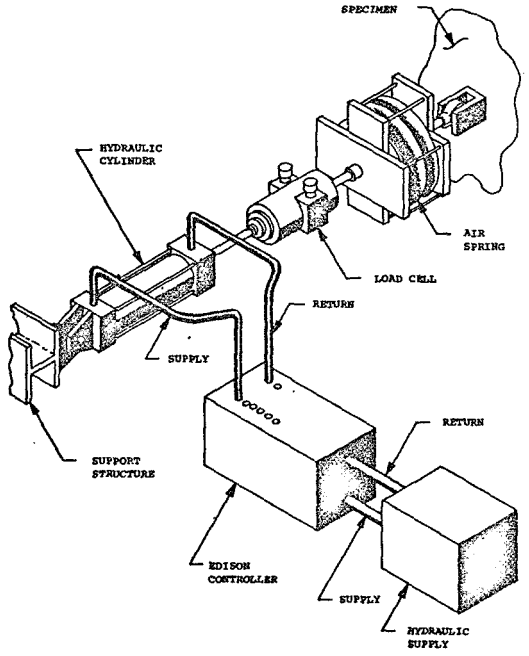

Figure 39. Schematic of Typical Static Loader

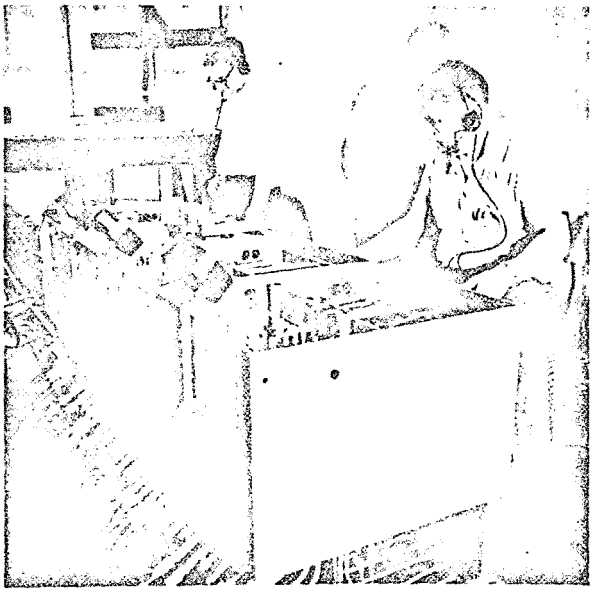

Figure 40. View of Hydraulic Static Load Maintainers

Air Bladders

The simulated aerodynamic loading requirement for the SLA surface is shown schematically in Figure 15. The required pressure distribution pattern was arbitrarily divided into 16 segments with each segment to receive the average air pressure required for that segment. The pressure distribution was such that nine pressures were required for controlling the bladders. Figure 23 shows schematically the negative pressure distribution required for the SIVB. The bladders for the SIVB were divided similarly to the SLA bladders, and also required nine control pressures. Accordingly, 18 channels of monitoring and control instrumentation were assembled. Figure 41 shows the pneumatic control schematic.

During the dynamics portion of the program, the SLA air bladders, even though they were 24 inches thick, would have contributed a significant amount of added stiffness to the SLA. To reduce this added stiffness to an acceptable magnitude, it was necessary to incorporate large reservoirs into the system in the form of external tanks, or plena, connected to each of the 32 SLA bladders.

Figure 42 illustrates the plena installed around the "Short Stack". The volume of each of the upper SLA bladders was 145 cu. ft. and the volume of the plenum connected to it was 725 cu. ft. The volume of the lower SLA bladder was 46 cu. ft. and the plenum was 230 cu. ft. To illustrate the effectiveness of the plena, consider the original stiffness of the SLA as 1. Adding the bladders to the system increased the apparent stiffness to 1.6. Adding the plena to the bladders resulted in an apparent stiffness of 1.1. To make the plena function effectively, it was necessary to have short length-large diameter connections, hence the plena were placed as close to the bladders as physically possible, and the connecting tubes were as large in diameter as the bird cage permitted. The connection between the bladders and the plena can be seen in Figure 43. Also, the lower plena can be seen. The design criteria for the tubular connections was to keep the Helmholz resonance above the dynamics test frequency. Test results showed that, with the 30 inch diameter and approximately 15 inch long connection, the Helmholz resonance was above 8.5 hz and highly damped.

For access reasons, the plena were not installed until the latter part of the program when the dynamic loads were applied.

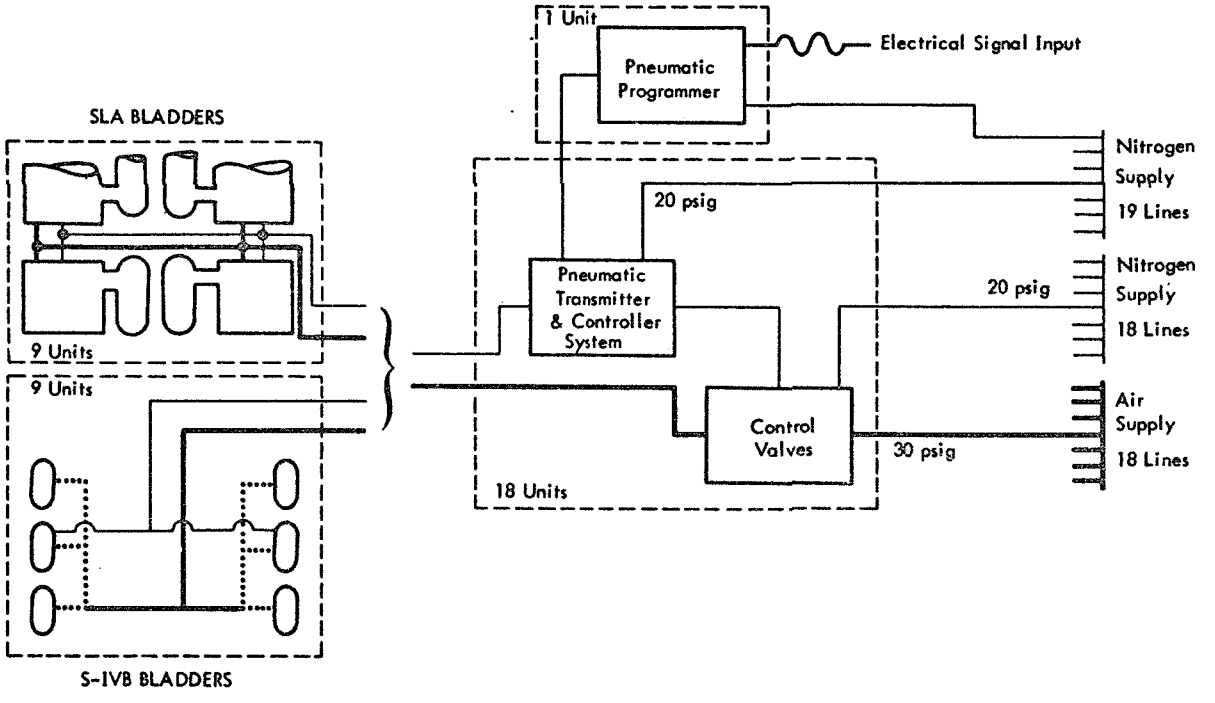

Figure 41. Schematic of Air Bladder Pneumatic Control

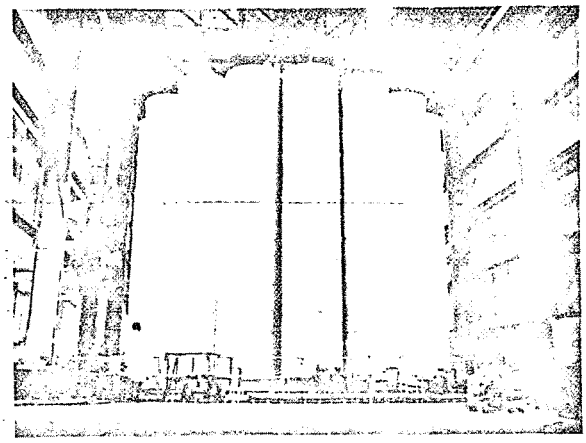

Figure 42. SLA Air Bladder Plena

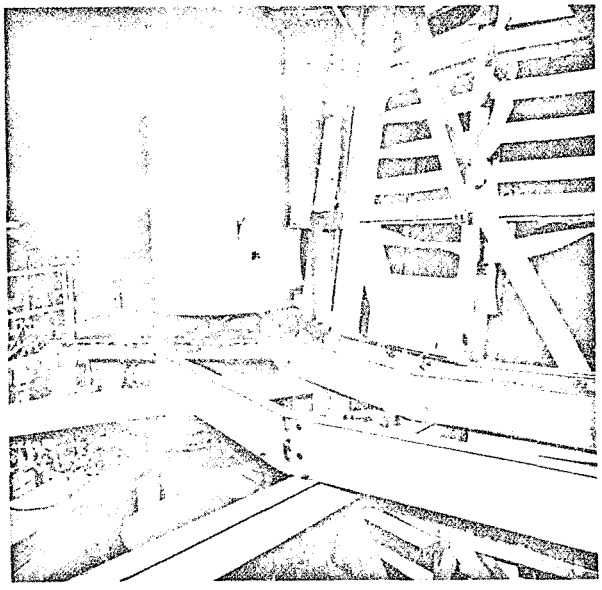

Figure 43. Connection Between SLA Air Bladder and Plenum

The air bladders inside the SIVB were about 40 inches thick, and the effective stiffness of the SIVB was greater than the SLA, and, therefore, plena were not considered necessary for the SIVB bladders.

Heater Control

The control of the power for the quartz lamps was accomplished as shown schematically in Figure 44. For control purposes, the lamps were divided into six zones, with each zone using a separate control thermocouple, Thermac Comparator, and Ignitron Power Controller. The power consumption for the lamps was so large that a special high voltage TVA power line was installed for the program.

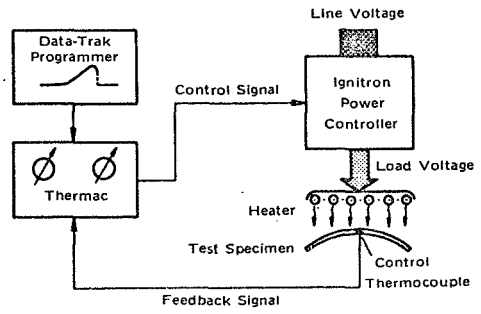

Figure 44. Schematic of Quartz Lamp Power Control

Dynamics Control

The dynamics control system was essentially that of the conventional hydrashaker which provided individual amplitude and phase control of the various shakers. Added to the control circuit was a force feedback loop with a differential pressure transducer sensing the hydraulic pressures on either side of the drive piston. This was done to achieve force stability, in addition to position stability. Figure 45 shows a control schematic for the shakers. The amplitude of the shaker force was manually controlled by adjusting the potentiometer until the desired response force level was displayed on the closed circuit TV screen. The most interesting facet of the control was how the force readout got to the TV screen. The LM is supported by four sets of four struts converging at the four apex fittings. Figure 46 shows the four struts at one of the apex fittings. Each of the sixteen struts was instrumented with strain gages to sense longitudinal force in the strut. These 16 signals were fed to the on-line computer which was programmed to convert these signals to three coordinates in terms of engineering units. The computer then added the coordinates from each of the four support points. It displayed, on a scope plotter, the three coordinate forces related to each support point, and the summation of forces in each coordinate axis. The scope plotter readout was relayed, by closed circuit TV, to the shaker operators console. The force data was upgraded once each second. The operator adjusted the shakers to control the summed forces in the axial and in the horizontal (Z) axis. The summation of response loads were adjusted to approximately 5800 lbs. peak in the axial direction and 3500 lbs. peak in the Z direction.

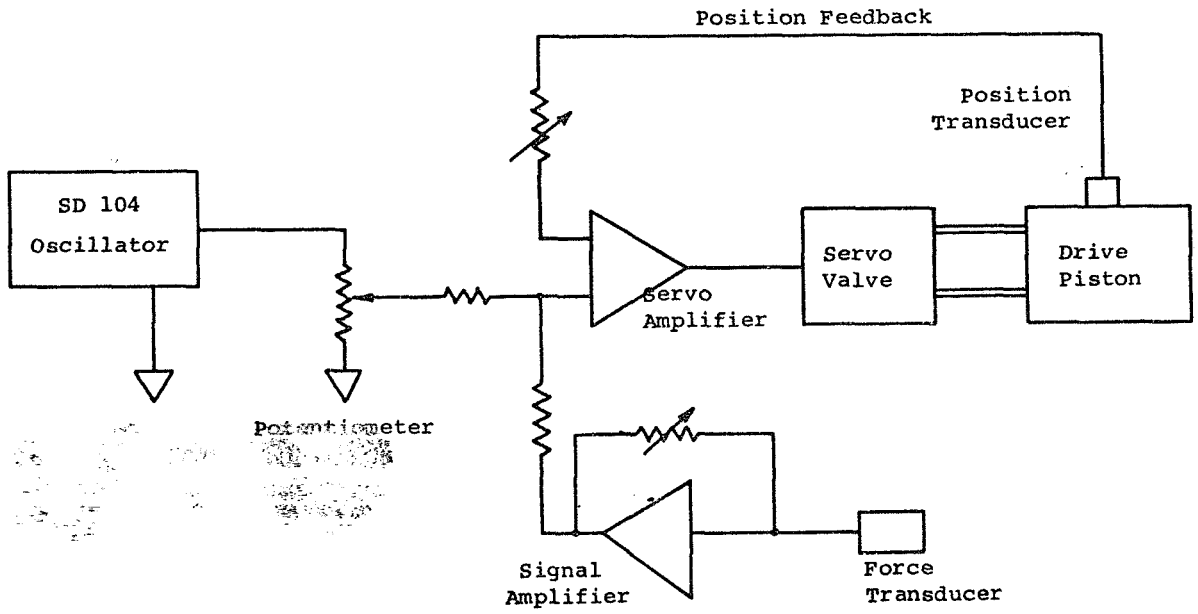

Figure 45. Schematic of Dynamic Loading Control

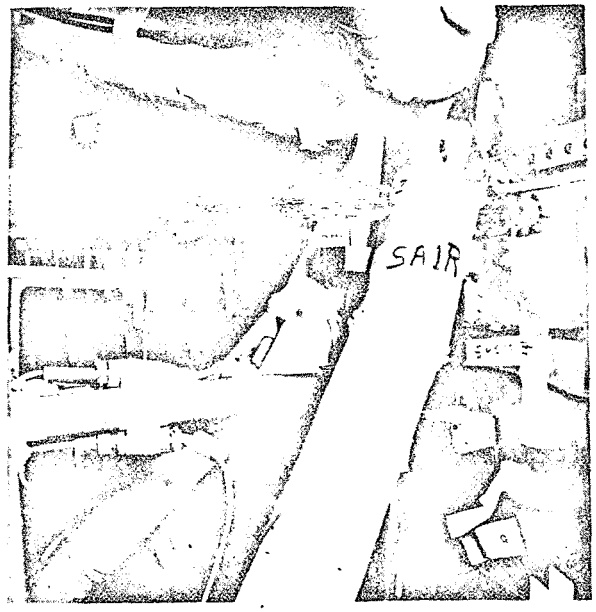

Figure 46. Lunar Module Apex Fitting and Struts

Abort System

In the event of a failure in any part of the test specimen or of a malfunction in any of the loading system it was necessary to be able to remove all the loads very quickly but with some degree of preset control. The test conductors consoles included an abort button which controlled all loading systems. To abort the hydraulically applied static loads, the abort circuit opened a solenoid valve in each of the Edison controllers which dumped the hydraulic pressure from all hydraulic cylinders. The static loads applied to the DCM and to the SM, high loads supplied with long hydraulic lines, would have taken far too long to dump through the Edison controllers, so solenoid dump valves were installed near to the actuators. These served to reduce the loads quickly, but due to the amount of oil flow required to drop the load the reduction took approximately one-half second.

To dump the air pressure in the SLA and SIVB air bladders, the abort circuit opened a solenoid in each bladder system, or, when the plena were installed, it opened a trap door in the bottom of each plenum. The size of the solenoids and the trap doors were selected to vent the bladders in approximately 1/2 second. To abort the heating system, the abort circuit simply turned off the controllers. The dynamic loads were not large enough to require automatic abort control.

DATA HANDLING

While not properly within the subject matter of this paper, data handling is, nonetheless, worthy of mention. Approximately 1600 channels of input and response data were fed to the on-line computer on a continuous basis. The computer corrected the data in accordance with previously stored calibration data, and converted it to engineering units. Twenty preselected channels were continuously displayed on the scope plotter. As each major point in the incremental loading pro-

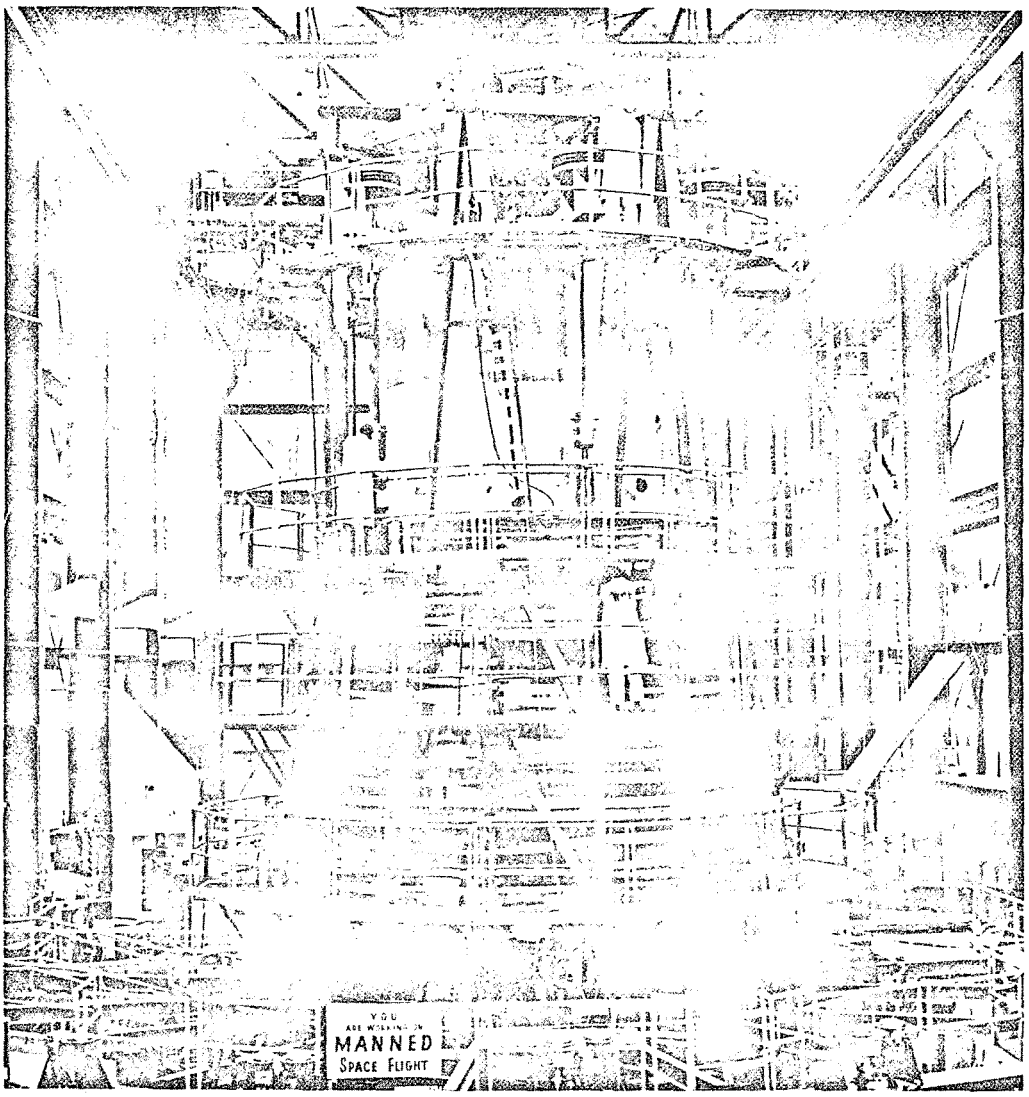

Figure 47. "Short Stack"

gram was reached, the computer was switched to the data dump mode. The computer then printed out the data in an organized format. The printed data was distributed to the data review team within three minutes of reaching the load point, and, normally within five minutes, the decision was reached to continue the loading program. More information on this phase of the program is presented in Reference 1.

CONCLUSIONS

The above floor level portion of the "Short Stack" is illustrated in Figure 47. Twenty seven feet of the stack is hidden below floor level. The entire setup, including the concept, design and fabrication of the test fixtures and restraint structures, was accomplished in 100 days. The test program required an additional 33 days.

The timely and successful completion of the test program represented a significant advancement in the state-of-the-art of combined environmental testing. This combination of loading had not previously been achieved on so large and complicated a structure. The short stack withstood all load conditions imposed without structural degradation.

REFERENCE

1. D. R. Reese and A. N. Levine, "Simulation of the Saturn V Boost-Phase Environment on Major Apollo Spacecraft Stages", I. E. S. Annual Meeting, May 1969.